

1 **Dual expansion routes likely underlie the present-day population structure in a**
2 ***Parnassius* butterfly across the Japanese Archipelago**

3

4 Hideyuki Tamura¹, Tomoaki Noda¹, Mikiko Hayashi¹, Yuko Fujii¹, Noriko Iwata¹, Yuko
5 Yokota¹, Masanori Murata¹, Chisato Tatematsu¹, Hideshi Naka^{1#}, Akio Tera, Katsumi
6 Ono, Kakeru Yokoi^{1\$}, Takanori Kato¹, Tomoko Okamoto¹, Koji Tsuchida^{1*}

7

8 1: Laboratory of Insect Ecology, Faculty of Applied Biological Sciences, Gifu
9 University, Yanagido 1-1, Gifu City, Gifu 501-1193, Japan.

10

11 [#]Present Address: The United Graduate School of Agricultural Sciences, Tottori
12 University, Koyama-Minami 4-101, Tottori City, Tottori 680-8553, Japan

13 ^{\$}Present Address: Insect Genome Research Unit, The National Agriculture and Research
14 Organization, Owashi 1-2, Tsukuba City, Ibaraki 305-8634, Japan

15

16 *: to whom correspondence should be addressed.

17

18 **Abstract**

19 The Japanese Archipelago, comprising a series of isolated yet interconnected islands,
20 had been geographically separated from the Eurasian continent. The linear topography
21 presents a unique biogeographic context for dispersing organisms from the continent. In
22 this study, we utilized mitochondrial DNA (mtDNA) and single nucleotide
23 polymorphism (SNP) variation to elucidate the dispersal history of the Japanese clouded
24 butterfly *Parnassius glacialis* across the Japanese Archipelago, including North Island
25 (Hokkaido), Main Island (Honshu) and Shikoku Island. Our analysis of mtDNA (COI,
26 COII) at 1192 base pairs (bps) revealed 49 haplotypes and identified three distinct
27 haplotype groups in the network. These groups correspond geographically to East
28 Japan, West Japan, and Chugoku-Shikoku. The Chugoku-Shikoku group is the most
29 ancient lineage. Interestingly, the Chugoku-Shikoku lineage showed a closer network
30 connection to the East Japan lineage than the geographically proximate West Japan
31 lineage. Divergence time estimates suggest that the Chugoku-Shikoku lineage diverged
32 from the continental *P. glacialis* approximately 3.05 million years ago (MYA).
33 Subsequently, from the Chugoku-Shikoku lineage, the East Japan and West Japan
34 lineages diverged around 1.05 MYA, with the subsequent divergence between the East
35 and West Japan lineages occurring at approximately 0.62 MYA. Based on the 3067 SNP
36 genotypes, population structure analysis revealed five distinct genetic structures within
37 the Japanese Archipelago, indicating geographical differentiation. From the analyses by
38 mtDNA and SNP variations, four primary genetic barriers were identified: between
39 Hokkaido and Honshu, between East and Central Japan, within the Kansai region, and
40 within the Chugoku region. The former three lines corresponded to the Blakiston Line,
41 the Itoigawa-Shizuoka Tectonic Line, and Lake Biwa, respectively. These findings

42 suggest that *P. glacialis* diverged from the continental *P. glacialis* and expanded its
43 range across the Japanese Archipelago via the North and South routes, establishing its
44 current distribution.

45

46 Keywords: phylogeography, *Parnassius*, Japanese Archipelago, mtDNA, SNP

47

48 1. Introduction

49 Evolutionary biological factors, including distances between individuals and
50 populations, stochastic events, and local population adaptations (e.g., Wright, 1943;
51 Nosil and Crespi, 2004; Nosil et al., 2005), reflect relatively recent events. On the other
52 hand, geological factors encompassing the formation of historical landforms reflect
53 considerably older events than the former (e.g., Otofuji et al., 1985; Jolivet et al., 1994;
54 Martin, 2011). The distribution of organisms is influenced by these two main factors,
55 resulting in their current distribution patterns. Indeed, organisms carry the history of
56 these influences.

57 The Proto-Japanese archipelago islands were located on the eastern edge of the

58 Eurasian continent until 20 million years ago (MYA), constituting the easternmost part
59 of the Eurasian continent. They originated from an accretionary wedge created by the
60 subduction of the oceanic plate beneath the continental plate (Nakajima, 2018).

61 According to the double-door hypothesis (Otofuji et al., 1985; Jolivet et al., 1994;
62 Martin, 2011), two half-arcs in the south-west and the north-east were later
63 differentiated and migrated from the continent, forming the Sea of Japan with them.
64 These half-arcs underwent opposing rotations and moved to their approximate positions,
65 separated by a valley known as Fossa Magna. This valley was later filled through

66 alluvial and volcanic activity at approximately 5 MYA, connecting the two half-arcs by
67 land and roughly forming the present-day outline of the Japanese Archipelago.

68 As the Japanese Archipelago is linearly connected from subarctic to subtropical
69 zones, species expansions into the Archipelago can be divided into two main routes
70 (Fig. 1). The first is from the West, which can be further divided into two sub-routes: via
71 the Korean Peninsula and the Ryukyu Archipelago. A land bridge connected eastern
72 China and western Japan continuously from the Late Miocene to the end of the Pliocene
73 (10–1.7 MYA; million years ago), allowing continuous immigration of continental
74 species into the Archipelago. Kitamura and Kimoto (2004) estimated the presence of a
75 land bridge between Kyushu and the continent at least 3.1 and 1.7 MYA, followed by
76 subsequent submergence.

77 In contrast, the North route is also divided into two sub-routes: one via
78 Sakhalin and the other via the Kuril Islands. The northern island of Hokkaido was
79 repeatedly connected to the continent during the Pleistocene, including the last glacial
80 periods (0.01–0.07 MYA, Fujimaki, 1994; Goto, 1994), with a land bridge between
81 Sakhalin and Hokkaido facilitating the immigration of many faunal species from the
82 continent. This land bridge is supported by evidence that the same phylogenetic insects
83 are distributed in both Hokkaido and Sakhalin (e.g., Sota and Hayashi, 2007; Hayashi
84 and Sota, 2014). Both the West and North routes are connected to the Eurasian
85 continent, and it is thought that part of the lineages differentiated on the Eurasian
86 continent spread and settled in the Japanese Archipelago. Occasionally, these lineages
87 are dispersed from the Japanese Archipelago back to the continent via these routes (Tojo
88 et al., 2017).

89 Species widely distributed across the Japanese Archipelago are excellent

90 subjects for elucidating the processes of their spread and exploring the mechanisms
91 underlying their local adaptation. Among these species, butterflies of the
92 genus *Parnassius* have attracted significant interest from researchers investigating their
93 dispersal from the continent and their migration routes. This genus originated on the
94 Tibetan Plateau and was initially adapted to alpine environments. It is believed that *P.*
95 *glacialis* differentiated as it adapted to lowland climates after experiencing a population
96 bottleneck in the lowlands of the continent (Si et al., 2020; Su et al., 2020; Tao et al.,
97 2020; Zhao et al., 2022, 2023; Tian et al., 2023).

98 *Parnassius glacialis* is a butterfly species distributed across Hokkaido
99 (Northern Island), Honshu (Main Island), and Shikoku Island in the Japanese
100 Archipelago. It was initially described as *P. glacialis* but has recently been referred as a
101 separate species, *P. citrinarius* without any supporting evidence (see supplementary
102 materials for the species name used in this study). Yagi et al. (2001) reported that
103 populations of both *P. citrinarius* (= *glacialis*) and *P. stubbendorfii* in Japan may have
104 been isolated from the continent on the Japanese islands during the early Pleistocene
105 glacial period (ca. 1.7-2.0 Ma). They noted that the genetic distance between the
106 Japanese *P. citrinarius* (= *glacialis*) and continental *P. glacialis* is substantial enough to
107 classify them as separate species compared to the genetic distances observed between
108 some other *Parnassius* species. Recently, Nagata (2024) also found that *P. citrinarius* (=
109 *glacialis*) shows differentiation between eastern and western Japan within the
110 Archipelago. However, the relatively small numbers of nucleotide sequences used in the
111 studies have limited the ability to further clarify the detailed degree of differentiation
112 and the expansion processes into the Japanese Archipelago.

113 This study aimed to analyze the DNA variations of *P. glacialis* in Japan to

114 estimate the dispersal process from the continent and the degree of variation within the
115 Japanese Archipelago. For this purpose, the COI and COII regions in the mitochondrial
116 DNA (mtDNA) were analyzed. These mtDNA analyses revealed that the Japanese
117 lineage can be divided into three main lineages. The relationship between these lineages
118 and the continental *P. glacialis* was also examined, and the divergence dates were
119 estimated using whole mtDNA genome sequencing. Furthermore, the recently
120 developed GRAS-Di method (Enoki and Takeuchi, 2018; Hosoya et al., 2019) was
121 employed to detect SNP loci in the species and to explore detailed population structure
122 based on these loci.

123

124 **2. Materials and Methods**

125 *2.1. Samples*

126 We collected the butterflies with an insect net and taken back to the laboratory.
127 Adult butterflies were collected at one to nine sites per prefecture, and the prefectural
128 units were treated as a single population in this study. Their wings were excised and
129 dried, while the remaining parts were stored in 100% ethanol (EtOH) at 4°C until DNA
130 extraction. All samples were collected from areas where this species is not banned from
131 collecting. From the samples, we selected 160 samples for 22 populations for SNP
132 analyses and 185 samples for 24 populations for mtDNA analyses. Samples for mtDNA
133 were collected in Fukui and Tochigi prefectures in addition to these sites for SNP
134 analyses. DNA was extracted from each sample as described below.

135 *2.2. Sequencing of mtDNA COI and COII*

136 DNA was extracted from two or three legs per specimen using a NucleoSpin®
137 Tissue kit (MACHEREY-NAGEL Düren, Germany). The isolated DNA was

138 resuspended in Tris-HCl buffer (pH 7.5) and stored at 4 °C. Polymerase chain reaction
139 (PCR) was conducted to amplify two gene regions: the contiguous mitochondrial
140 cytochrome oxidase I (COI) region of 721 base pairs (bps) and cytochrome oxidase II
141 (COII) region of 470 bps. Primers to amplify the COI region were JNfwd (5'-
142 GCAGGAACCTGGATGAACAG-3') and Krev (5'-GAGTATCGTCGAGGTATCC-3')
143 (Dechaine et al., 2004). Primers used to amplify the COII region were PierreIII (5'-
144 AGAGAGTTCACCTTAATAGAAC-3'; Nazari et al., 2007) and Eva (5'-
145 GAGAACATTACTGCTTCAGTCATCT-3'; Bogdanowicz et al., 1993). Both
146 fragments were amplified using TaKaRa Ex Taq Hot Start Version (TaKaRa, Tokyo,
147 Japan). PCR conditions for the COI region were 94°C for 5 min, followed by 30 cycles
148 of 94°C for 30 s, 50°C for 30 s, and 72°C for 1 min. For the COII region, 95°C for 5
149 min, followed by 35 cycles of 94°C for 1 min, 50°C for 1 min, 72°C for 1 min, and
150 finally 72°C for 10 min. Sequencing reactions were performed using BigDye terminator
151 v3.1 (Applied Biosystems, Carlsbad, USA). All samples were sequenced using an ABI
152 PRISM 3100-Avant Genetic Analyzer (Applied Biosystems, Carlsbad, CA, USA).
153 Sequencing was conducted at the Life Science Experimental Center and Genome
154 Research Department, Gifu University. PCR fragments were sequenced in both
155 directions to ensure accuracy. The sequences were aligned the sequences using MEGA
156 6.06 (Tamura et al., 2013).

157 We estimated population demography using a Bayesian skyline plot by BEAST
158 v.2.7.6 (Drummond et al., 2006; Drummond & Rambaut, 2007). Nucleotide diversity,
159 haplotype diversity, Fu's F, and Tajima's D were estimated by Arlequin 3.5.2.2
160 (Excoffier and Lischer 2010).

161 *2.3. Whole Genome Sequencing of mtDNA for Three Lineages*

162 Our COI and COII analyses revealed that *P. glacialis* across the Japanese
163 Archipelago is broadly divided into the East Japan, West, and Chugoku-Shikoku
164 lineages (see Results). Therefore, three representative individuals were selected from
165 these three lineages (the East Japan from Hokkaido, West Japan from Shiga, and
166 Chugoku-Shikoku from Kochi), and DNA was extracted from the thoraxes of these
167 specimens. Extraction was carried out using the previously mentioned kit, following the
168 manufacturer's protocol. After DNA extraction, the following analyses were conducted
169 at a commercial sequencing facility (Bioengineering Lab Co., Ltd., Kanagawa, Japan).
170 Libraries were prepared according to the manual using the MGIEasy FS DNA Library
171 Prep Set (MGI Tech). Following the provided manual, Cyclized DNA was prepared
172 from the library and the MGIEasy Circularisation Kit (MGI Tech). DNBs were prepared
173 according to the manual using the DNBSEQ-G400RS High-throughput Sequencing Kit
174 (MGI Tech). Sequencing analysis of the produced DNBs was performed using the
175 primer supplied with the High-throughput Pair-End Sequencing Primer Kit (App-D)
176 (MGI Tech) and DNBSEQ-G400 (MGI Tech) platform at 2x150 bp. After removing
177 adapter sequences using Cutadapt v. 4.0 (Martin, 2011), Sickle v. 1.33 (Joshi and Fass,
178 2011) was used to remove bases with a quality score of less than 20 and paired reads
179 with less than 75 bases. SPAdes v. 3.15.5 (Bankevich et al. 2012) was used to assemble
180 high-quality reads with the following parameters: a lower limit of read coverage (--cov-
181 cutoff = 10) and mismatch correction (-careful). Mitochondrial sequences were
182 extracted from the assembled sequences using Metaxa v. 2.2 (Bengtsson-Palme et al.,
183 2015) .

184 Adapter trimming and low-quality read removal were performed with
185 Trimmomatic v.0.39 (Bolger et al., 2014). Sequence assembly was performed using

186 GetOrganelle v.1.7.7.1 (Jin et al., 2020). Alignment of these sequences together with the
187 continental *Parnassius* sequences yielded a dataset of 15,185 bp, including indels
188 (accession number = submitting).

189 *2.4. SNP Detection*

190 SNPs were detected from the extracted DNA using the GRAS-Di method. Enoki
191 and Takeuchi (2018) presented the protocol at a conference, and Hosoya et al. (2019)
192 subsequently published the detailed procedure. This protocol constructs libraries using
193 two sequential PCR steps like MIG-seq (Suyama and Matsuki 2015). The first PCR
194 primers consist of 10 bases of Illumina Nextera adaptor 3'-end sequences plus 3-base
195 random oligomers (13 bases). The final PCR product is purified using columns or
196 magnetic beads without size selection and then applied for sequencing on an Illumina
197 platform. GRAS-Di has the advantages of simplicity in library construction and the
198 ability to detect many SNPs. Libraries were prepared using the 2nd-step tailed PCR
199 method; primers for 1st and 2nd PCR were followed by Hosoya et al. (2019). Cyclized
200 DNA was prepared according to the manual using the produced library and the
201 MGIEasy Universal Library Conversion Kit (App-A, MGI Tech). DNA Nanoballs
202 (DNB) were prepared using the DNBSEQ DNB Rapid Make Reagent Kit (MGI Tech)
203 and High-Throughput Pair-End Sequencing Primer Kit (App-D, MGI Tech), following
204 the provided manuals. Sequencing was performed using DNBSEQ-T7RS High-
205 throughput Sequencing Kit (MGI Tech) with the primer supplied with the High-
206 Throughput Pair-End Sequencing Primer Kit (App-D) and DNBSEQ-T7 (MGI Tech)
207 platform at a 2x150 bp condition. To remove primer sequences, the first three bases of
208 each read were removed using Cutadapt v. 4.0 (Martin, 2011). Paired reads with a
209 quality score of less than 30 and less than 75 bases were filtered out using Sickle v.1.33

210 (Joshi and Fass, 2011). Sequences after 75 nucleotides were retained to standardize read
211 length for data analysis. The raw fastq sequence data of each sample were deposited
212 into NCBI Sequence Read Archive (Supplemental Table 2).

213 Subsequently, *denovo_map.pl* of Stacks v. 2.62 (Catchen et al., 2013) was
214 executed with the following parameters: minimum number of reads required to form a
215 stack ($m = 5$), maximum number of nucleotide differences allowed between stacks for
216 merging ($M = 2$), maximum number of nucleotide differences allowed when building
217 the catalog ($n = 2$), and assembly using paired-end reads ($--paired$). The SNPs
218 information was obtained by running the program with the following settings: $n = 2$
219 (maximum number of nucleotide differences allowed when merging stacks) and
220 assembly using paired end reads. These analyses were conducted at the commercial
221 sequencing facility.

222 *2.5. Phylogeographic Analyses*

223 For COI and COII data, phylogenetic trees were constructed using the neighbor-
224 joining (NJ) (Saitou & Nei, 1987), maximum likelihood (ML), and Bayesian inference
225 (BI) methods. NJ trees were generated using MEGA X (Kumar et al. 2018) with the *p*-
226 distance method. ML trees were constructed with RAxML (Stamatakis, 2014), and BI
227 trees were built with MrBayes v.3.1.2 (Ronquist & Huelsenbeck, 2003). Bootstrap
228 testing was conducted with 1,000 trials for the NJ and ML trees. ML analysis was
229 performed using each model for each gene codon and assessed using Akaike
230 information criterion (AIC) scores in Modeltest2 v. 2.3 (Nylander, 2004), and the
231 selected model was HKY + I + G4. Similarly, BI was performed using each model for
232 each gene codon and assessed using AIC scores in Kakusan4 (Tanabe, 2011), and the
233 selected model was HKY + I + G. We aligned the sequences of 185 adults. As

234 outgroups, we used the continental *Parnassius* sequences: *Parunassius glacialis* in
235 China (NC 065029_1), *P. stubbendorfii* (OP 709281_1), *P. orleans* (NC 072335_1), and
236 *P. epaphus* (NC 026864_1). Haplotype networks were obtained with TCS v. 1.21
237 (Clement et al., 2000).

238 For whole mtDNA sequence data, phylogenetic trees were constructed using the
239 neighbor-joining (NJ) (Saitou & Nei, 1987), maximum likelihood (ML), and Bayesian
240 inference (BI) methods. NJ trees were generated using MEGA X (Kumar et al. 2018)
241 with the *p*-distance method. ML trees were constructed with RAxML (Stamatakis,
242 2014), and BI trees were built with MrBayes v.3.1.2 (Ronquist & Huelsenbeck, 2003).
243 Bootstrap testing was conducted with 1,000 trials for the NJ and ML trees. ML analysis
244 was performed using each model for each gene codon and assessed using Akaike
245 information criterion (AIC) scores in Modeltest2 v. 2.3 (Nylander, 2004), and the
246 selected model was TIM2 + G4. Similarly, BI was performed using each model for each
247 gene codon and assessed using AIC scores in Kakusan4 (Tanabe, 2011). The selected
248 model was GTR + G. We aligned the sequences of three adults of the three
249 representative lineages (East Japan, West Japan, and Chugoku-Shikoku). As outgroups,
250 we used the continental *Parnassius* sequences; *Parunassius glacialis* in China (NC
251 065029_1), *P. stubbendorfii* (OP 709281_1), *P. orleans* (NC 072335_1), and *P. epaphus*
252 (NC 026864_1), *P. acdestis* (NC 072544_1), *P. hide* (NC 072287_1), *P. cephalus* (NC
253 026457_1), *P. simo* (NC 072286_1).

254 We estimated divergence times using BEAST v. 2.7.6 (Drummond et al., 2006;
255 Drummond & Rambaut, 2007) with 10,000,000 generations of Markov-chain Monte
256 Carlo iterations, sampled every 1,000 generations under a relaxed clock model with an
257 uncorrelated lognormal distribution. Here, we used the HKY + G model and three

258 calibration time points according to Si et al. (2020). The calibrations for the molecular
259 dating were based on two butterfly fossils: *Praepapilio colorado* Durden (Papilionidae)
260 from the Green River Shale of Colorado (USA) of mid-Eocene early Lutetian age (41–
261 48 MYA) and *Thaites ruminiana* Scudder (subfamily Parnassiinae) from Aix-en-
262 Provence (southern France) of late Oligocene Chattian age (23–28 MYA) (Durden and
263 Rose 1978, Jong 2017, Condamine et al. 2018); thus, the crown group divergence of the
264 Parnassiinae was constrained between 23 MYA and 48 MYA. The earliest divergence
265 time of seven *Parnassius* subgenera other than *P. epaphus*, exclusive of
266 subgenus *Parnassius* was set to be 16–37 Ma.

267 *2.6. SNP Data Analysis*

268 We used STRUCTURE v. 2.0 (Pritchard et al., 2000) to delineate the number of
269 genetically identified clusters (K) and assign individuals to clusters without prior
270 information on their origin population. We calculated an *ad hoc* criterion of ΔK (Evanno
271 et al., 2005) for determining the optimal K value using STRUCTURE Harvester (Earl &
272 Holdt, 2012). The assignment index for each individual in each population was
273 calculated using the CLUMPAK server (Kopelman et al., 2015). Genetic variation
274 associated with various hierarchical levels of populations and their fixation index (F)
275 values were quantified using analysis of molecular variance (AMOVA; Excoffier et al.,
276 1992) in GenoDive ver. 3.0. (Meirmans, 2020). We conducted principal component
277 analysis (PCA) using GenoDive v. 3.0.

278 We used Netview R v.1.0 operated by R v.4.2.3 (Neuditschko et al. 2012; Steinig
279 et al. 2016) to reveal fine-scale population stratification independent of *a priori* ancestry
280 information. We generated a population network based on a shared allele distance
281 matrix (1-identity by state (IBS)) generated with PLINK v.1.9. The network was

282 visualized by R v.4.2.3. We also used TreeMix v.1.13 (Pickrell and Pritchard, 2012) to
283 investigate patterns of population splits and cross-population gene flow.

284

285 **3. Results**

286 *3.1. Phylogeography*

287 We detected and aligned COI (721 bps) and COII (470 bps) for each individual
288 (accession number = in submitting). Although, if the samples in Okayama were
289 generally included in the Chugoku Region were put into West Japan (Haplotype 06),
290 three distinct clusters were identified in the Haplotype network by TCS (Fig. 2),
291 corresponding to the West Japan, East Japan, Chugoku-Shikoku respectively.

292 Demography statistics were calculated for the three strains, and the Chugoku-Shikoku
293 strain showed a trend towards higher nucleotide diversity than the other strains (Table
294 S1). Fu's *F* values were significantly negative in the West Japan and East Japan
295 lineages, while Tajima's *D* was not significantly negative, suggesting a weak tendency
296 towards population expansion. On the other hand, neither value was negative for the
297 Chugoku-Shikoku lineage. Skyline plots showed recent population increases in West
298 Japan and the Chugoku -Shikoku lineage (Fig. S1) but not in the East Japan lineage.

299 The three phylogenetic trees could be combined into one consensus tree (Fig. 3).
300 There, the posterior probability and bootstrap value for the branching of the Chugoku-
301 Shikoku lineage were highest, from which the East Japan and West Japan lineages
302 diverged. A clear difference between the three phylogenetic trees was the position of the
303 continental *P. glacialis*. The position of the continental *P. glacialis* was out of Japanese
304 lineages in NJ (Fig. S2). However, the ML and BI trees contained that position within
305 the Japanese lineages (Fig. S3 and 3).

306 The continental *P. glacialis* was included within *P. glacialis* in Japan, so the
307 phylogenetic tree was rebuilt using the whole mtDNA sequences of the continental
308 *Parnassius* species and those of three lineages of *P. glacialis* in Japan (accession
309 number = in submitting) by the three phylogenetic methods and Beast. The consensus
310 tree (Fig. S4) showed the continental *P. glacialis* located outside *P. glacialis* in Japan,
311 which was derived from the continental *P. glacialis*, which was supported with high
312 probability (1/100/100: BI/ML/NJ). The oldest lineage of *P. glacialis* in Japan was the
313 Chugoku-Shikoku lineage (Fig. 4), which was supported with a high probability
314 (1/100/100). *P. glacialis* in Japan diverged from the continental *P. glacialis* at 3.05
315 MYA ; after that, the remaining the East Japan and West Japan lineages diverged at 1.05
316 MYA, showing again that the Chugoku-Shikoku lineages were most ancestral ones
317 across the Japanese Archipelago. The East Japan and West Japan lineages diverged at
318 0.62 MYA.

319 *3.2. Population structure depicted by SNPs*

320 We detected 3067 SNP loci using a method of GRAS-Di (Enoki and Takeuchi,
321 2018; Hosoya et al., 2019) and analyzed with STRUCTURE based on the information
322 of those loci for 160 individuals. The results showed that ΔK (Evanno et al., 2005) for
323 determining the optimal K value using STRUCTURE Harvester (Earl & Holdt, 2012)
324 was highest at $K = 5$, which was the most appropriate cluster number (Fig. 5). Four clear
325 genetic clusters were found at $K = 5$: Hokkaido and Tohoku (dark blue), Koshinetsu
326 (blue), Chubu (white) and Shikoku (orange)—in the case of $K = 6$, a new cluster
327 appeared in Shizuoka, indicating that the populations across the Japanese Archipelago
328 were divided into eastern and western Japan, with Shizuoka as the boundary.

329 The results analyzed by NetviewR were consistent with those of STRUCTURE

330 (Fig. 6). Characteristically, Hokkaido was isolated with the Blakiston Line between
331 Hokkaido and Honshu (main Island), and the Kansai was divided into two groups. One
332 group of the Kansai was connected to the Chugoku, while the other was connected to
333 the Chubu. Individuals from the Kansai connected to the Chugoku were collected from
334 the western shore side of Lake Biwa to Hyogo prefecture. In contrast, those from the
335 Kansai connected to the Chubu were collected from the eastern shore side of Lake Biwa
336 to Toyama prefecture, with Lake Biwa acting as one geographical barrier. Another clear
337 barrier was found between the northern regions (Tohoku, Koshinetsu, and Chubu) and
338 the central regions (Chubu and Kansai).

339 The individuals from the Chubu connected to those of the Kansai, including
340 those collected in northern Gifu and Toyama prefectures. The other individuals of the
341 Chubu were connected to those of the Koshinetsu and Tohoku and included individuals
342 from southern Gifu and Shizuoka. The individuals from Sado Island in the Sea of Japan
343 were not connected to the individuals from Niigata, where it is administratively
344 included, but rather to those from the Tohoku. These results were generally consistent
345 with the Treemix results (Fig. S5).

346 The PCA results were consistent with the STRUCTURE and NetviewR results
347 (Fig. S6). Hokkaido and Shizuoka prefectures were located separately, and the three
348 populations in the Shikoku region also formed a single cluster.

349

350 **4. Discussion**

351 We revealed that *P. glacialis* in Japan was divided into three distinct genetic
352 lineages in mtDNA of COI + COII analyses: East Japan, spanning from Hokkaido to the
353 Koshinetsu region; West Japan, spanning Chubu to the Chugoku region; and the

354 Chugoku-Shikoku region. The results of the SNP analyses generally supported these
355 genetic structures. Of particular interest is that the Chugoku-Shikoku lineage was
356 estimated to have the oldest branching time. Furthermore, the Haplotype network
357 showed that the East Japan lineage was connected to the Chugoku-Shikoku lineage
358 rather than the geographically closer West Japan lineage (Fig. 2).

359 In the phylogenetic trees with the continental *Parnassius* species as the
360 outgroup, three clusters were generally identified in the trees from the three methods
361 (Fig. 3). However, phylogenetic relationships other than the Chugoku-Shikoku lineage
362 were unclear in the ML method (Fig. S3). Despite this, all phylogenetic trees suggested
363 that the Chugoku-Shikoku lineage diverged first. The phylogenetic tree based on 1192
364 bp of mtDNA sometimes showed the continental *P. glacialis* included within the
365 phylogenetic tree of *P. glacialis* in Japan, but this issue was resolved using the whole
366 mtDNA sequence (Fig. S4). Our branching time estimates indicate that *P. glacialis* in
367 Japan diverged from the continental *P. glacialis* approximately 3.05 MYA, with the two
368 remaining lineages diverging at 1.05MYA from the Chugoku-Shikoku lineage,
369 confirming that the Chugoku-Shikoku lineage is the most ancestral across the Japanese
370 Archipelago. Furthermore, the haplotype network demonstrated that the East Japan
371 lineage is linked to the Chugoku-Shikoku lineage rather than to the geographically
372 closer West Japan lineage (Fig. 2). These results suggest that the East Japan lineage may
373 have been derived from the Chugoku-Shikoku lineage, followed by the divergence of
374 the West Japan lineage from the East Japan lineage.

375 Our results show that (1) the Chugoku-Shikoku lineage is the oldest lineage, and
376 (2) the East Japan lineage is linked to the Chugoku-Shikoku lineage rather than to the
377 geographically closer West Japan lineage. Two routes have been postulated for the

378 expansion of biota distribution in the Japanese Archipelago: A North route and a West
379 route (Fig. 1). Let us now consider two scenarios in which the distribution is expanded
380 from one of these routes. For example, if we assume that the East Japan lineage
381 expanded its distribution from the North route and then derived the West Japan lineage
382 and the Chugoku-Shikoku lineage, the Chugoku-Shikoku lineage would be the most
383 recent lineage. This would be inconsistent with our data, which indicates that the
384 Chugoku-Shikoku lineage was the oldest.

385 Let us also consider another scenario in which the Chugoku-Shikoku lineage
386 expanded its distribution from the West route, from which the West Japan and East
387 Japan lineage were subsequently derived. In this scenario, the most ancestral Chugoku-
388 Shikoku lineage would be closely related to the West Japan lineage, which would also
389 be inconsistent with our data. In other words, assuming a single route would not resolve
390 the discrepancy with our data. The most appropriate route to resolve these discrepancies
391 is a scenario in which two routes have been followed. Namely, the oldest Chugoku-
392 Shikoku lineage expanded into the Japanese Archipelago via the West route. In contrast,
393 the East Japan lineage, which is phylogenetically most closely linked to it, expanded its
394 distribution into the Japanese Archipelago via the North route. The scenario in which
395 the West Japan lineage diverged from the East Japan lineage in the Japanese
396 Archipelago is the scenario that can explain our data without contradiction. In other
397 words, this species is thought to have differentiated from the continental *P. glacialis* in
398 mainland China, expanded its distribution in the Japanese Archipelago via two routes,
399 and formed a contact zone in the central mainland (Honshu).

400 Organisms that have differentiated traits and phylogeny from east to west within
401 the Japanese Archipelago have been known, and it has been suggested that they may

402 have expanded their distribution in the Japanese Archipelago via two routes, one to the
403 North and the other to the West (Suzuki et al., 1996, 2002; Yoshimura et al., 2001;
404 Schoville et al., 2013; Hayashi and Sota, 2014). However, neither of these phenomena
405 has been confirmed by phylogeography. The present data are the first results supporting
406 the two-route hypothesis.

407 SNP analyses with the GRAS-Di detected 3067 loci. STRUCTURE analysis
408 indicated $K = 5$ was the most appropriate population number. Four clusters were
409 identified at $K = 5$ (Fig. 5): Hokkaido/Tohoku (dark blue), Koshinetsu (blue), Chubu
410 (white), and Shikoku (orange). These populations are connected from the north to the
411 south of the Japanese Archipelago, and these boundaries may act as barriers to gene
412 flow.

413 Fig. 7 compares the boundaries of the clusters as identified from mtDNA (A)
414 and SNP (B). The mtDNA results observed two clear barriers (a and b). One barrier (b)
415 corresponds well to the Itoigawa-Shizuoka Tectonic Line, which marks the western end
416 of the Fossa Magna. The other barrier divides the area, including Shikoku region and
417 Hiroshima prefectures, from the area further east. The former barrier is known to divide
418 organisms east and west of this line in other species, and geohistorical influences have
419 been repeatedly noted (Suzuki et al., 1996, 2002; Yoshikawa et al., 2001). Conversely,
420 the latter barrier corresponds to the boundary between Hiroshima and Okayama
421 Prefectures, but it has not been previously identified as a biological boundary.

422 In contrast, five genetic clusters with four barriers (i to iv in Fig. 7B) were
423 identified in the nuclear genes of SNPs: (1) Hokkaido, (2) Tohoku, (3) East Chubu
424 including Koshinetsu and South Chubu, (4) Hokuriku including Toyama, north Gifu and
425 East of Shiga, (5) West Japan including West Kansai, Chugoku, and Shikoku. A closer

426 examination reveals that barrier (i) runs through the central part of Kansai and is
427 associated with the boundary at Lake Biwa. The areas between barriers (i) and (ii)
428 include Toyama, northern Gifu, and the eastern shore of Lake Biwa in Shiga. Southern
429 Gifu Prefecture, however, shows greater connectivity with the Koshinetsu region
430 between barriers (ii) and (iii). Historically, the northern and southern administrative
431 regions of Gifu Prefecture differed, and natural conditions remain distinct even today.
432 This phenomenon is also observed in another butterfly, *Luehdorfia japonica*, where
433 mtDNA haplotypes from the Chubu to the Kansai region are relatively complex and
434 intricately intermingled in a relatively narrow range (Suzuki et al., 2023). Thus, this
435 distribution may reflect gene flows through relatively recent human activity rather than
436 geohistorical influences.

437 The combined map of barriers in Fig. 7C shows an area where the three mtDNA
438 and SNP lineages are contacting. The area enclosed by the dotted square indicates this
439 contact zone. In allopatric and parapatric speciation, the post-branching contact of
440 divergent lineages is termed secondary contact (Coyne and Orr, 2004). Here, we used
441 this term to denote the situation where different lineages of the same species are in
442 contact. Comparing the distribution regions of mtDNA (A) and SNP (B) genotypes,
443 SNP (B) is more finely divided. Upon closer examination, we can recognize areas of
444 discrepancy between the two markers. For instance, the position of line (a) in mtDNA
445 differs from that of line (i) in SNP (B). Additionally, line (b) of mtDNA is situated
446 between lines (ii) and (iii) of SNPs. This indicates that individuals entering these two
447 regions belong to the same group for SNPs, but to different groups for mtDNA. This
448 indicates that SNPs are spreading across mtDNA boundaries, suggesting that the
449 spreading nature of the gene is faster for SNPs than for mtDNA.

450 The triangles in Fig 7C illustrate that from the red line of the mtDNA lineage
451 boundary, there is a nuclear gene expansion towards the blue line of the SNP boundary.
452 This indicates that the gene flow from the boundary (a) to the east opposes the gene
453 flow direction from the boundary (b) to the west, which corresponds to the boundary of
454 Lake Biwa. In other words, nuclear gene flow directions appear to conflict within the
455 contact zone. The biological significance of the Lake Biwa boundary is currently
456 unknown but will be an area of future investigation.

457 A feature of this result is the difference in the degree of introgression between
458 nuclear DNA and mtDNA: the triangles in Fig. 7C indicate regions of greater
459 introgression of nuclear DNA than mtDNA. A factor that may contribute to this
460 difference in the introgression of nuclear DNA and mtDNA is activity differences
461 between males and females. The behavior of organisms can be divided into two types:
462 male philopatry, where males tend to stay in their territories, and female philopatry,
463 where females tend to remain in their territories (Greenwood, 1980). In the case of
464 butterflies, including this species, most exhibit female philopatry, and the sex ratio of
465 actively flying adults is generally skewed toward males. In this case, nuclear DNA
466 would be expected to spread more easily.

467 SNP analysis indicates that the Chugoku-Shikoku lineage appears to have been
468 extending eastward. In contrast, the East Japan lineage seems to have been expanding
469 westward across the Sea of Japan in the past. This suggests that the two lineages
470 currently come into contact around Lake Biwa. If this scenario holds, Haldane's law
471 (Coyne and Orr 2004) may be observed, where heterozygous individuals, particularly
472 females in Lepidopteran insects, are more disadvantaged when hybridizing. However,
473 data from amateur entomologists indicate no significant mortality increases were

474 observed when mating individuals from distant collecting sites (Ono and Tera, personal
475 communication). On the other hand, anecdotal evidence suggests that *P. glacialis* in
476 Japan mates with the continental *P. glacialis* to produce viable offspring. If confirmed,
477 this implies that reproductive isolation between the two lineages between China and
478 Japan is not well operating and warrants careful consideration in future studies.

479 The present study demonstrates that *P. glacialis* colonized Japan via North and
480 West routes to the Japanese Archipelago. While previous studies (e.g., Hayashi and
481 Sota, 2014) inferred this dual-route entry, it has been genetically confirmed in this study.
482 Despite undergoing long-distance migration across the Sea of Japan via these two
483 routes, there appears to be no apparent fertility deficit in the contact zone. This study
484 provides insights into the species' distant history of this species. Future research on
485 adaptive genes will be crucial for understanding their recent and future evolutionary
486 trajectories.

487 **5. Conclusion**

488 The results of this study indicate that *Parnassius glacialis* in Japan differentiated
489 from the continental *P. glacialis* and subsequently migrated to the Japanese Archipelago
490 via two expansion routes: a West route and a North route. The most ancestral lineage
491 entered the Japanese Archipelago via the West route, while its derived lineages spread
492 via the North route. The lineage derived from the North route and the lineage from the
493 West route are thought to be currently in contact in the central part of the Japanese
494 Archipelago. Within the contact zone of these two lineages, differences in the
495 distribution of nuclear genes and mtDNA were observed, suggesting that female
496 philopatry is one of the contributing factors.

497

498 **Acknowledgments**

499 We thank T. Takeda, N. Nagahama, T. Takeuchi, M. Kawada, H. Matsuno, A. Yokokura,
500 T. Kudo, J. Ogasawara for their sample collection and providing samples.

501

502 **References**

503 Bankevich, A., Nurk, S., Antipov, D., Gurevich, A.A., Dvorkin, M., Kulikov, A.S.,
504 Lesin, V.M., Nikolenko, S.I., Pham, S., Prjibelski, A.D., Pyshkin, A.V., Sirotkin,
505 A.V., Vyahhi, N., Tesler, G., Alekseyev, M.A., Pevzner, P.A., 2012. SPAdes: A
506 New Genome Assembly Algorithm and Its Applications to Single-Cell
507 Sequencing. *Journal of Computational Biology* 19, 455–
508 477. <https://doi.org/10.1089/cmb.2012.0021>

509 Bogdanowicz, S.M., Wallner, W.E., Bell, J., Odell, T.M., Harrison, R.G., 1993. Asian
510 gypsy moths (Lepidoptera: Lymantriidae) in North America: evidence from
511 molecular data. *Annals of the Entomological Society of America* 86, 710–715.
512 <http://doi.org/10.1006/mpev.1999.0744>

513 Bolger, A.M., Lohse, M., Usadel, B., 2014. Trimmomatic: a flexible trimmer for
514 Illumina sequence data. *Bioinformatics* 30, 2114–2120.
515 <https://doi.org/10.1093/bioinformatics/btu170>

516 Catchen, J., Hohenlohe, P.A., Bassham, S., Amores, A., Cresko, W.A., 2013. Stacks: an
517 analysis tool set for population genomics. *Molecular Ecology* 22, 3124–3140.
518 <http://doi.org/10.1111/mec.12354>

519 Clement, M., Posada, D., Crandall, K.A., 2000. TCS: a computer program to estimate
520 gene genealogies. *Molecular Ecology* 9, 1657–1659.

521 Condamine, F.L., Rolland, J., Höhna, S., Sperling, F.A.H., Sanmartín, I., 2018. Testing

522 the role of the Red Queen and Court Jester as drivers of the macroevolution of
523 Apollo butterflies. *Systematic Biology* 67, 940–964.
524 <http://doi.org/10.1098/rsbl.2014.1049>

525 Coyne, J.A., Orr, H.A., 2004. *Speciation*. Sinauer, Sunderland, UK.

526 De Jong, R., 2017. Fossil butterflies, calibration points and the molecular clock
527 (Lepidoptera: Papilioidea). *Zootaxa* 4270, 1–63.

528 Drummond, A., Ho, S., Phillips, M., Rambaut, A., 2006. Relaxed phylogenetics and
529 dating with confidence. *PLoS Biology* 4, e88.
530 <http://doi:10.1371/journal.pbio.0040088>

531 Drummond, A., Rambaut, A., 2007. BEAST: Bayesian evolutionary analysis by
532 sampling trees. *BMC Evolutionary Biology* 7, 214. <http://doi:10.1186/1471-2148-7-214>

533 Durden, C.J., Rose, H., 1978. Butterflies from the middle Eocene: the earliest
534 occurrence of fossil Papilioidea (Lepidoptera). The earliest occurrence of fossil
535 Papilioidea (Lepidoptera). Texas Memorial Museum, The University of Texas
536 at Austin.

537 Earl, D., vonHoldt, B., 2012. STRUCTURE HARVESTER: a website and program for
538 visualizing STRUCTURE output and implementing the Evanno method.
539 *Conservation Genetics Resources* 4, 359–361. <http://dx.doi.org/10.1007/s12686-011-9548-7>

540 Enoki, H., Takeuchi, Y., 2018. New genotyping technology, GRAS-Di, using next
541 generation sequencer. *Plant and Animal genome conference XXVI*.

542 Evanno, G., Regnaut, S., Goudet, J., 2005. Detecting the number of clusters of
543 individuals using the software STRUCTURE: a simulation study. *Molecular*

546 Ecology 14, 2611–2620. <http://doi.org/10.1111/j.1365-294X.2005.02553.x>

547 Excoffier, L., Smouse, P.E., Quattro, J.M., 1992. Analysis of molecular variance
548 inferred from metric distances among DNA haplotypes: application to human
549 mitochondrial DNA restriction data. Genetics 131, 479–491.

550 Excoffier, L., Lischer, H.E.L., 2010. Arlequin suite ver 3.5: a new series of programs to
551 perform population genetics analyses under Linux and Windows. Molecular
552 Ecology Resources 10, 564–567. <http://dx.doi.org/10.1111/j.1755-0998.2010.02847.x>

553 Fujimaki, Y., 1994. Across the strait: fauna of mixture. In: Ishigaki, K., Fukuda, M.
554 (Eds.), Formation history of nature of Hokkaido. Hokkaido University Press,
555 Sapporo, pp. 167-179.

556 Goto, A., 1994. Fishes in rivers and lakes: origin and adaptive strategy. In: Ishigaki, K.,
557 Fukuda, M. (Eds.), Formation history of nature of Hokkaido. Hokkaido University
558 Press, Sapporo, pp. 150-166.

559 Greenwood, P.J., 1980. Mating systems, philopatry, and dispersal in birds and
560 mammals. Animal Behaviour 28, 1140–1162.

561 Hayashi, M., Sota, T., 2014. Quaternary donaciine beetles (Coleoptera, Chrysomelidae)
562 in Japan: Colonization and divergence patterns inferred from fossil and molecular
563 data. Quaternary International 341, 255–266.
564 <https://doi.org/10.1016/j.quaint.2013.08.022>

565 Hosoya, S., Hirase, S., Kikuchi, K., Nanjo, K., Nakamura, Y., Kohno, H., Sano, M.,
566 2019. Random PCR-based genotyping by sequencing technology GRAS-Di
567 (genotyping by random amplicon sequencing, direct) reveals genetic structure of
568 mangrove fishes. Molecular Ecology Resources 19, 1153–1163.

570 <https://doi.org/10.1111/1755-0998.13025>

571 Jolivet, L., Tamaki, K., Fournier, M., 1994. Japan Sea, opening history and mechanism:

572 A synthesis. *Journal of Geophysical Research: Solid Earth* 99, 22237–22259.

573 <https://doi.org/10.1029/93JB03463>

574 Joshi, N.A., Fass, J.N., 2011. Sickle: A sliding-window, adaptive, quality-

575 based trimming tool for FastQ files

576 (Version 1.33) [Software]. Available at <https://github.com/najoshi/sickle>

577 Kitamura, A., Kimoto, K., 2004. Reconstruction of the Akihisa Southern Channel of the

578 Japan Sea at 3.9-1.0 Ma. *Quaternary Research* 43, 417–434 (in Japanese with

579 English summary). <http://doi.org/10.4116/jaqua.43.417>

580 Kopelman, N.M., Mayzel, J., Jakobsson, M., Rosenberg, N.A., Mayrose, I., 2015.

581 Clumpak: a program for identifying clustering modes and packaging population

582 structure inferences across K. *Molecular Ecology Resources* 15, 1179–1191.

583 <https://doi.org/10.1111/1755-0998.12387>

584 Kumar, S., Stecher, G., Li, M., Knyaz, C., Tamura, K., 2018. MEGA X: Molecular

585 Evolutionary Genetics Analysis across Computing Platforms. *Molecular Biology*

586 and Evolution

35, 1547–1549. <https://doi.org/10.1093/molbev/msy096>

587 Martin, A.K., 2011. Double saloon door tectonics in the Japan Sea, Fossa Magna, and

588 the Japanese Island Arc. *Tectonophysics* 498, 45–65.

589 <https://doi.org/10.1016/j.tecto.2010.11.016>

590 Martin, M. (2011). Cutadapt removes adapter sequences from high-throughput

591 sequencing reads. *EMBnet.journal* 17, 10–

592 12. <https://doi.org/10.14806/ej.17.1.200>

593 Meirmans, P.G., 2020. genodive version 3.0: Easy-to-use software for the analysis of

594 genetic data of diploids and polyploids. *Molecular Ecology Resources* 20, 1126–
595 1131. <https://doi.org/10.1111/1755-0998.13145>

596 Nagata, N., 2024. Phylogeography of *Parnassius citrinarius* based on mitochondrial
597 DNA reveals large differences in genetic structure between the Eastern and
598 Western Japan. *Zoological Science* 41. <https://doi.org/10.2108/zs230072>

599 Nakajima, K., 2018. Tectonics of sedimentary basins in and around Japan since the
600 opening of the Sea of Japan. *Journal of the Geological Society of Japan* 124, 693–
601 722 (in Japanese with English summary).
602 <http://doi.org/10.5575/geosoc.2018.0049>

603 Nazari, V., Zakharov, E.V., Sperling, F.A.H., 2007. Phylogeny, historical biogeography,
604 and taxonomic ranking of Parnassiinae (Lepidoptera, Papilionidae) based on
605 morphology and seven genes. *Molecular Phylogenetics and Evolution* 42, 131–
606 156. <https://doi.org/10.1016/j.ympev.2006.06.022>

607 Neuditschko, M., Khatkar, M.S., Raadsma, H.W., 2012. NetView: A high-definition
608 network-visualization approach to detect fine-scale population structures from
609 genome-wide patterns of variation. *PLoS ONE* 7, e48375.
610 <http://doi.org/10.1371/journal.pone.0048375>

611 Nosil, P., Crespi, B.J., 2004. Does gene flow constrain adaptive divergence or vice
612 versa? a test using ecomorphology and sexual isolation in *Timema cristinae*
613 walking-sticks. *Evolution* 58, 102–112. <http://doi.org/10.1111/j.0014-3820.2004.tb01577.x>

615 Nosil, P., Vines, T.H., Funk, D.J., 2005. Reproductive isolation caused by natural
616 selection against immigrants from divergent habitats. *Evolution* 59, 705–719.
617 <http://doi.org/10.1111/j.0014-3820.2005.tb01747.x>

618 Nylander, J.A.A., 2004. MrModeltest v2. Program distributed by the author.

619 Otofuji, Y.-I., Matsuda, T., Nohda, S., 1985. Opening mode of the Japan Sea inferred
620 from the palaeomagnetism of the Japan Arc. *Nature* 317, 603–604.

621 <http://doi.org/10.1038/317603a0>

622 Pickrell, J., Pritchard, J., 2012. Inference of population splits and mixtures from
623 genome-wide allele frequency data. *PLoS Genetics*, e1002967.

624 <http://doi.org/10.1371/journal.pgen.1002967>

625 Pritchard, J.K., Stephens, M., Donnelly, P., 2000. Inference of population structure using
626 multilocus genotype data. *Genetics* 155, 945–959.

627 Ronquist, F., Huelsenbeck, J.P., 2003. MrBayes 3: Bayesian phylogenetic inference
628 under mixed models. *Bioinformatics* 19, 1572–1574.

629 <http://doi.org/10.1093/bioinformatics/btg180>

630 Saitou, N., Nei, M., 1987. The neighbor-joining method: a new method for
631 reconstructing phylogenetic trees. *Molecular Biology and Evolution* 4, 406–425.

632 <http://doi.org/10.1093/oxfordjournals.molbev.a040454>

633 Schoville, S.D., Uchifune, T., Machida, R., 2013. Colliding fragment islands transport
634 independent lineages of endemic rock-crawlers (Grylloblattodea: Grylloblattidae)
635 in the Japanese Archipelago. *Molecular Phylogenetics and Evolution* 66, 915–927.

636 <https://doi.org/10.1016/j.ympev.2012.11.022>

637 Si, C., Chen, K., Tao, R., Su, C., Ma, J., Li, L., Hao, J., Yang, Q., 2020. Genetic
638 differentiation and divergence time of Chinese *Parnassius* (Lepidoptera:
639 Papilionidae) species based on nuclear internal transcribed spacer (Its) sequence
640 data. *Journal of Entomological Science* 55, 520–546.

641 <http://doi.org/10.18474/0749-8004-55.4.520>

642 Sota, T., Hayashi, M., 2007. Comparative historical biogeography of *Plateumaris* leaf
643 beetles (Coleoptera: Chrysomelidae) in Japan: interplay between fossil and
644 molecular data. *Journal of Biogeography* 34, 977–993.
645 <https://doi.org/10.1111/j.1365-2699.2006.01672.x>

646 Stamatakis, A., 2014. RAxML version 8: a tool for phylogenetic analysis and post-
647 analysis of large phylogenies. *Bioinformatics* 30, 1312–1313.
648 <http://doi.org/10.1093/bioinformatics/btu033>

649 Steinig, E.J., Neuditschko, M., Khatkar, M.S., Raadsma, H.W., Zenger, K.R., 2016.
650 netview p: a network visualization tool to unravel complex population structure
651 using genome-wide SNPs. *Molecular Ecology Resources* 16, 216–227.
652 <https://doi.org/10.1111/1755-0998.12442>

653 Su, C., Xie, T., Wang, Y., Si, C., Li, L., Ma, J., Li, C., Sun, X., Hao, J., Yang, Q., 2020.
654 Miocene diversification and high-altitude adaptation of *Parnassius* butterflies
655 (Lepidoptera: Papilionidae) in Qinghai–Tibet Plateau revealed by large-scale
656 transcriptomic data. *Insects* 11, 754. <http://doi.org/10.3390/insects11110754>

657 Suyama, Y., Matsuki, Y., 2015. MIG-seq: an effective PCR-based method for genome-
658 wide single-nucleotide polymorphism genotyping using the next-generation
659 sequencing platform. *Scientific Reports* 5, 16963.
660 <http://doi.org/10.1038/srep16963>

661 Suzuki, H., Sato, Y., Fujiyama, S., Ohba, N., 1996. Allozymic differentiation between
662 two ecological types of flashing behavior in the Japanese firefly, *Luciola cruciata*.
663 *Japanese Journal of Entomology* 64, 682–691.

664 Suzuki, H., Sato, Y., Ohba, N., 2002. Gene diversity and geographic differentiation in
665 mitochondrial DNA of the Genji firefly, *Luciola cruciata* (Coleoptera:

666 Lampyridae). *Molecular Phylogenetics and Evolution* 22, 193–205.

667 <http://dx.doi.org/10.1006/mpev.2001.1046>

668 Suzuki, S., Suzuki, T., Shibuya, Y., Goto, M., Yokoyama, J., Kato, T., Ando, M.,

669 Okamoto, T., Tsuchida, K., 2023. Expansion processes of two emblematic

670 Luehdorfia butterflies across the Japanese Archipelago. *Journal of Biogeography*

671 50, 1710–1723. <https://doi.org/10.1111/jbi.14682>

672 Tamura, K., Stecher, G., Peterson, D., Filipski, A., Kumar, S., 2013. MEGA6:

673 Molecular Evolutionary Genetics Analysis Version 6.0. *Molecular Biology and*

674 *Evolution* 30, 2725–2729. <http://doi.org/10.1093/molbev/mst197>

675 Tanabe, A.S., 2011. Kakusan4 and Aminosan: two programs for comparing

676 nonpartitioned, proportional and separate models for combined molecular

677 phylogenetic analyses of multilocus sequence data. *Molecular Ecology Resources*

678 11, 914–921. <https://doi.org/10.1111/j.1755-0998.2011.03021.x>

679 Tao, R., Xu, C., Wang, Y., Sun, X., Li, C., Ma, J., Hao, J., Yang, Q., 2020.

680 Spatiotemporal differentiation of alpine butterfly *Parnassius glacialis*

681 (Papilionidae: Parnassiinae) in China: Evidence from mitochondrial dna and

682 nuclear single nucleotide polymorphisms. *Genes* 11, 188.

683 <https://doi.org/10.3390/genes11020188>

684 Tian, X., Mo, S., Liang, D., Wang, H., Zhang, P., 2023. Amplicon capture

685 phylogenomics provides new insights into the phylogeny and evolution of alpine

686 *Parnassius* butterflies (Lepidoptera: Papilionidae). *Systematic Entomology* 48,

687 571–584. <https://doi.org/10.1111/syen.12591>

688 Tojo, K., Sekiné, K., Takenaka, M., Isaka, Y., Komaki, S., Suzuki, T., Schoville, S.D.,

689 2017. Species diversity of insects in Japan: Their origins and diversification

690 processes. *Entomological Science* 20, 357–381. <http://doi.org/10.1111/ens.12261>

691 Wright, S., 1943. Isolation by distance. *Genetics* 28, 114–138.

692 Yagi, T., Katoh, T., Chichvarkhin, A., Shinkawa, T., Omoto, K., 2001. Molecular
693 phylogeny of butterflies *Parnassius glacialis* and *P. stubbendorfii* at various
694 localities in East Asia. *Genes & Genetic Systems* 76, 229–234.
695 <http://doi.org/10.1266/ggs.76.229>

696 Yoshikwa, T., Ide, K., Kubota, Y., Nakamura, Y., Takebe, H., Kusaoka, H., 2001.
697 Intraspecific genetic variation and molecular phylogeny of *Luciola cruciata*
698 (Coleoptera: Lampyridae) inferred from the mitochondrial ND5 gene sequences.
699 *Japanese Journal of Entomology* 4, 117–127 (in Japanese with English summary).
700 http://doi.org/10.20848/kontyu.4.4_117

701 Zhao, Y., He, B., Tao, R., Su, C., Ma, J., Hao, J., Yang, Q., 2022. Phylogeny and
702 biogeographic history of *Parnassius* butterflies (Papilionidae: Parnassiinae) reveal
703 their origin and deep diversification in West China. *Insects* 13, 406.
704 <http://doi.org/10.3390/insects13050406>

705 Zhao, Y., Su, C., He, B., Nie, R., Wang, Y., Ma, J., Song, J., Yang, Q., Hao, J., 2023.
706 Dispersal from the Qinghai-Tibet plateau by a high-altitude butterfly is associated
707 with rapid expansion and reorganization of its genome. *Nature Communications*
708 14, 8190. <http://doi.org/10.1038/s41467-023-44023-2>

709

710 **Author contributions: CrediT**

711 H.N., A.T., K.O., T.O and K.T. conceived the study; H.T., T.N., M.H., Y.F., N.I., Y.Y.,
712 M.M., C.T., H.N., A.T., K.O., and K.T. collected the samples and extracted DNA. H.T.,
713 T.N. M.H., Y.F., N.I., Y.Y., M.M., and C.T. analysed genetic variation of mtDNA; K.Y,

714 T.K., T.O., and K.T. conducted data analyses; K.T. wrote the manuscript; all authors
715 approved the final version of the manuscript.

716

717 **Conflicts of interest**

718 The authors declare that they have no competing interests.

719

720 **Data accessibility**

721 All genetic and related data used in the analyses will be deposited in Dryad.

722

723

724 **Legends of figures**

725 Fig 1. The outline of the present-day Japanese Archipelago and expected biological
726 expansion routes from the Eurasian continent, North and West routes. The regional
727 names are shown in bold, and prefecture names cited in the text were also shown.
728 Circles and squares indicate each collection site for SNP analyses in this study. Samples
729 for mtDNA were collected in Fukui and Tochigi prefectures in addition to these sites.
730

731 Fig. 2. Haplotype network depicted by TCS using the sequences of 49 haplotypes
732 detected in *Parnassius glacialis* in Japan. Each number was the haplotype number.
733

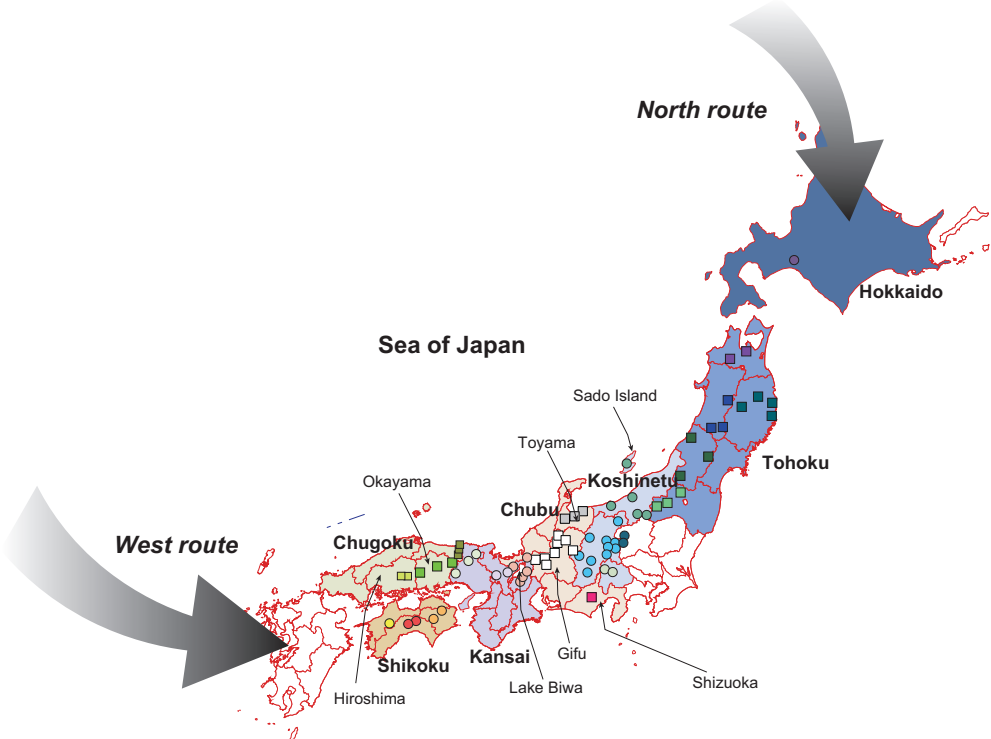
734 Fig. 3. A consensus tree of BI (Bayesian Inference), ML (Maximum Likelihood), and NJ
735 (Neighbor Joining) methods. The tree was the result of BI method. The values above
736 each branch showed the posterior probability of BI, the bootstrap value of ML, and that
737 of NJ, respectively. The values less than 0.6 of posterior probability and 60 of bootstrap
738 value were not shown in this figure. The bold letters indicated the haplotype numbers.
739

740 Fig. 4. Bayesian estimates of the divergence time obtained using BEAST ver. 2.7.6.
741 under HKY + G model, using whole mtDNA sequences of nine species and the three
742 lineages of *P. glacialis* in Japan. The values around each node indicate the estimated
743 divergence time. Horizontal bars indicate the 95% credible age interval at each node,
744 with a posterior probability 1. The representative sequences for the West Japan, East
745 Japan, and Chugoku-Shikoku lineages were obtained from the samples collected in
746 Shiga, Hokkaido, and Kochi prefectures.
747

748 Fig. 5. Population assignment using STRUCTURE from $K = 3$ to 9. Each population
749 (prefecture) and regional name (in bold letters) were shown in the bottom margin from
750 North (left) to South (right).
751

752 Fig. 6. The result of NetviewR using SNPs variations. Each line showed the connection
753 of each genotype.
754

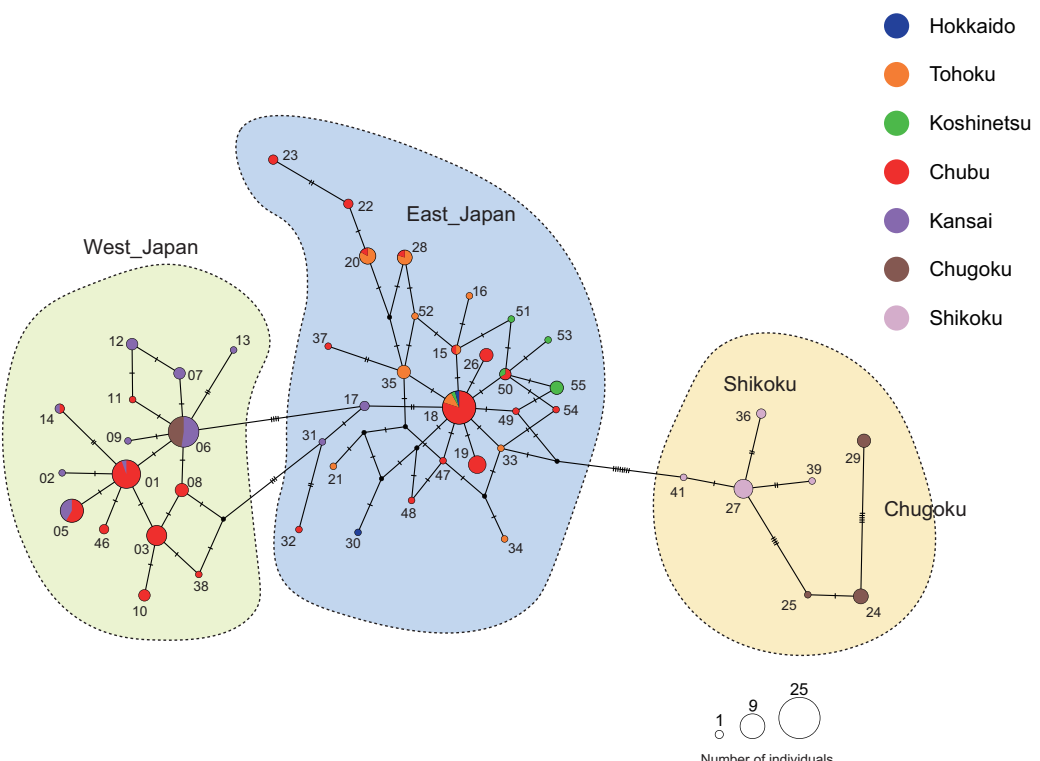
755 Fig. 7. Population barriers estimated by (A) mtDNA, (B) SNP analyses. Our estimated
756 combined barriers were shown in (C). The dotted rectangle shows inferred contact zone
757 among the lineages.
758
759



760

761 Fig. 1.

762

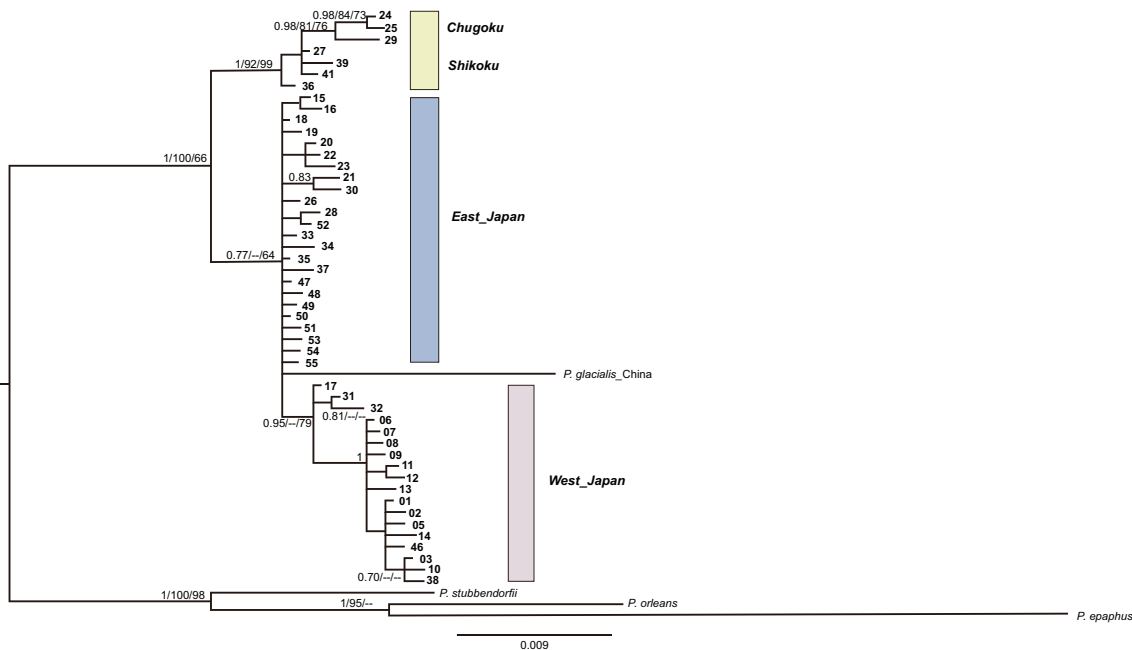


763

764 Fig. 2.

765

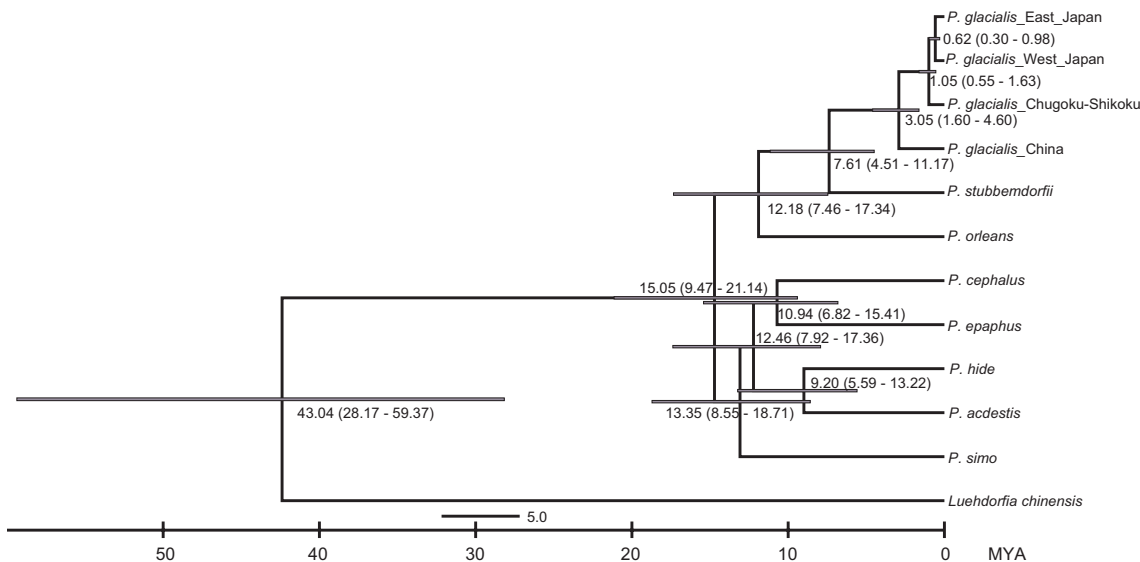
766



767

768 Fig. 3

769

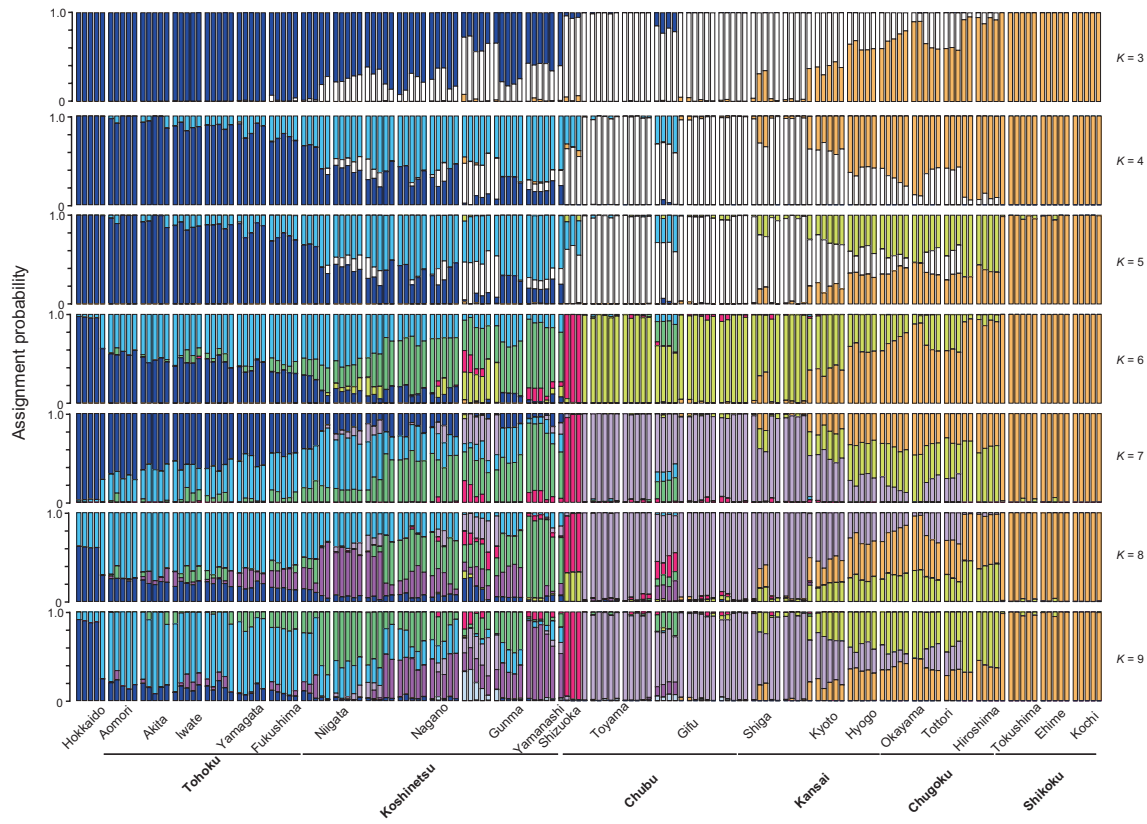


770

771 Fig. 4

772

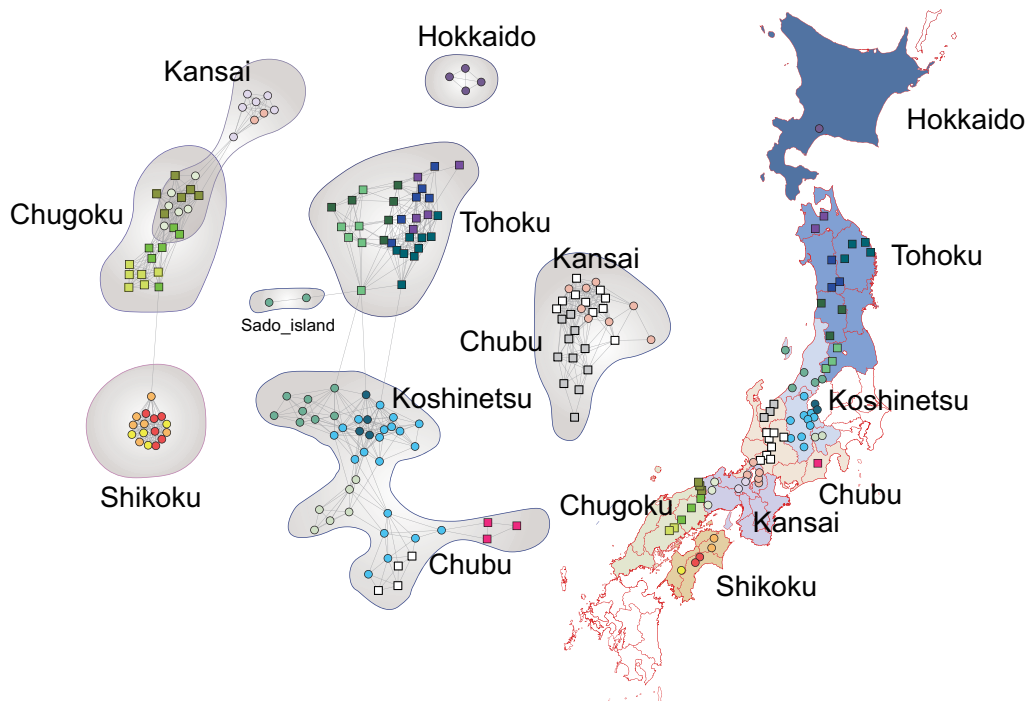
773



774

775 Fig. 5

776



777

778 Fig. 6

